Hydrogen–air turbulent flame propagation in the presence of microdroplets

S P Medvedev, S V Khomik, O G Maximova, G L Agafonov, V N Mikhalkin and A S Betev

Semenov Institute of Chemical Physics of the Russian Academy of Sciences, Kosygina 4, Moscow 119991, Russia

E-mail: s_p_medvedev@chph.ras.ru

Abstract. A technique has been developed for evaluating turbulent combustion characteristics in the presence of microdroplets obtained by vapor condensation in the course of rapid expansion. Experiments have been conducted to visualize spark-initiated flame propagation through hydrogen–air mixtures at various turbulent intensities, water-vapor volume fractions, and microdroplet concentrations.The influence of microdroplet suspensions on iginition and flame propagation is investigated.

1. Introduction

Ignition and flame propagation can occur in a mixture of a hydrogen-containing fuel, an oxidizer, water vapor, and microdroplets (mist) after a reactive two-phase medium is created as a result of rapid expansion of an initially homogeneous saturated vapor–gas system.

Microdroplet mist formation by expansion of a saturated vapor is substantially different from mechanical dispersion (liquid spraying) in terms of both mechanism and technical aspects. Numerous liquid atomization methods using spray nozzles have been reviewed in [1] and other publications. Whereas the smallest Sauter mean diameter (SMD) obtained by these methods varies between 10 and 20 μm and wide droplet size distributions are observed because of coalescence, condensation of an expanding vapor gives rise to a cloud of monodisperse droplets (mist) with size on the order of 1 μm. The resulting two-phase system should be clearly distinguished from the misty fog commonly found in nature. Natural fog arises when the air contains suspended condensation nuclei, such as dust grains [2]. Under these conditions, the smallest droplet size varies between 10 and 30 μm. Mist is formed in the course of expansion as a result of transition from an initially homogeneous vapor state to a metastable state, followed by homogeneous droplet nucleation.

Vapor condensation caused by rapid expansion has long been a focus of experimental shock-wave studies because one of the main components of a conventional shock tube is a high-pressure (driver) section, where a compressed gas undergoes an isentropic expansion.

The kinetics of condensation in rarefaction waves generated in shock tubes have been addressed in [3–8]. The most systematic approach to this problem was developed by Glass with co-workers [5–7], who analyzed both experimental data and theoretical aspects of two basic mechanisms of droplet formation (heterogeneous and homogeneous nucleation). An important

contribution was made by Hastings and Hodson [8], who performed two-color light transmission measurements to investigate microdroplet growth dynamics.

Over the past 25 years, extensive research on the subject has been done by the van Dongen group at the Eindhoven University of Technology [9–12]. In particular, it was shown in [11, 12] that the high-pressure section, where condensation occurs, can be used as a fine-resolution device for studying droplet nucleation and growth. This was made possible by designing a shock tube with a local widening in the low-pressure section. An advanced light-transmission technique was employed where measurements were performed at three wavelengths [13] to evaluate not only SMD but also the droplet size variance and the droplet number density.

An analysis of results presented in [5–12] shows that rapid expansion of vapor–gas systems is an effective means for creating a gas–microdroplet/mist two-phase mixture. Consider a system where a combustible carrier gas is mixed with water microdroplets. After the gas is ignited, the flame propagates through a two-phase mixture where water mist acts as an inhibitor because of heat loss by droplet evaporation. It is important that the droplet number density can be varied over a wide range by adjusting the initial conditions (vapor density, temperature, and pressure at the start of the expansion). This makes it possible to determine characteristics of flame–droplet interaction and investigate the effect of the liquid phase on the flammability limits of the carrier gas.

Inert liquid (mostly water) spraying systems are used to prevent and suppress fires caused by methane outbursts in coal mines [13, 14]. After the accidents at Three Mile Island Nuclear Generating Station (1979, USA) and Chernobyl Nuclear Power Plant (1986, USSR), large-scale programs were initiated to investigate the explosion hazard characteristics of hydrogen–air mixtures. Addition of inert gases (CO_2, N_2) or water vapor to a hydrogen-containing reactive mixture has been explored among other measures to prevent explosions [15–20]. Studies of the flammability limits of diluted hydrogen-air mixtures have shown that the concentration of triatomic molecules (CO_2 or H_2O) required to suppress ignition and subsequent flame propagation amounts to 60 vol % [16–19], while the concentration of nitrogen to be added is 70 vol % [19, 20]. The addition of quantities as high as these may have a negative effect due to an increase in total pressure rise in the venting volume.

In an alternative approach free of this disadvantage, a liquid (water) is sprayed to form a cloud of microdroplets. It was demonstrated in [21–23] that the flammability limits of hydrogen–air mixtures are narrower in the presence of a condensed phase. It was found that the inhibiting effect strongly depends on the droplet size in the spray. When the droplet size was between 20 and 50 μm (volume fraction was 10^{-3}), the lower flammability limit shifted insignificantly, from 4 vol % of hydrogen in air (in the absence of droplets) to 4.5–5.3 vol %. With droplet size reduced to 10 μm, the lower flammability limit was 7.2 vol % of hydrogen at 20 °C and 8.5 vol % at 70 °C. Smaller droplets could not be obtained under the experimental conditions of [22, 23] because of the limitations of mechanical dispersion mentioned above. This makes the use of rapid expansion to create droplets of size no larger than 2 μm a promising approach in terms of enhancing the inhibiting effect of water mist.

The study of such systems requires an experimental technique that combines measurement of the evolution of a gas–droplet mixture in the course of expansion with investigation of ignition and flame propagation, with particular focus on control of droplet size and concentration. These requirements were met in the design of the experimental setup used in this study. The design and operating principles of the setup, as well as the transition from a homogeneous hydrogen–air–vapor system to a heterogeneous mixture of hydrogen, air, water vapor, and microdroplets, were described in [24]. The setup was used to determine the flammability limits of hydrogen–air mixtures in the presence of water microdroplets (mist) [25]. Experiments have shown that microdroplets of size no larger than 2 μm obtained by vapor condensation in the course of rapid expansion not only compensate for vapor loss from the system but also effectively

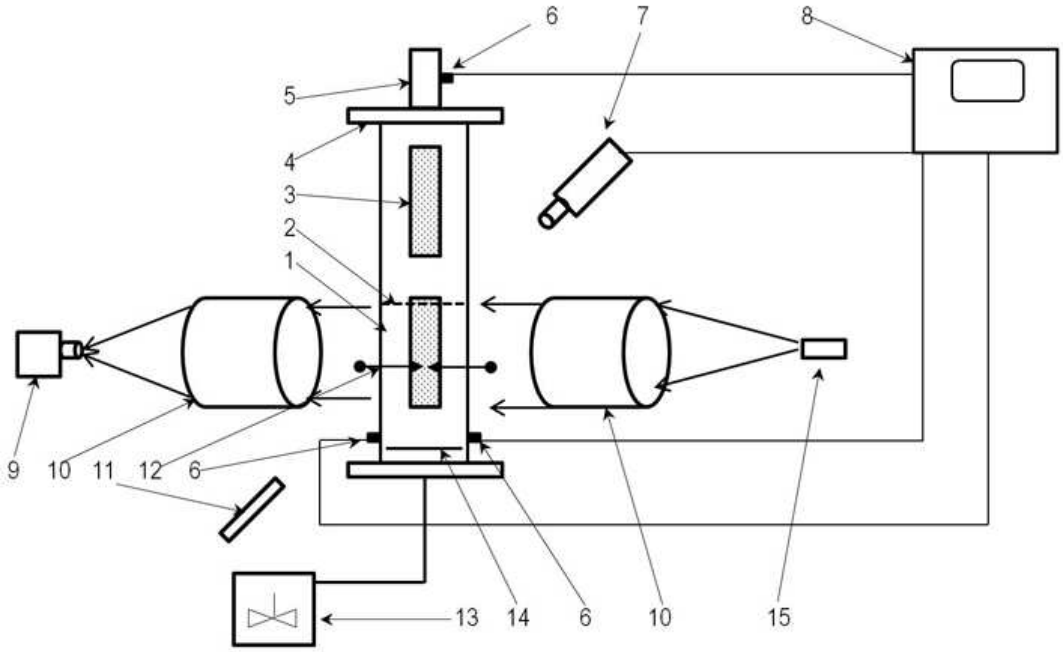

Figure 1. Experimental setup: *1*—preheated combustion chamber; *2*—perforated plate; *3*—quartz window; *4*—flange; *5*—gas outlet; *6*—pressure transducer; *7*—photodetector; *8*—digital data acquisition and processing system; *9*—Mikrotron-1362 high-speed camera; *10*—Telemar-2 telephoto lens; *11*—IR laser diode; *12*—spark gap; *13*—mixer; *14*—blank plate; *15*—point light source.

suppress explosions of hydrogen–air mixtures. Partial vapor condensation results in a narrower flammability range.

However, our previous studies did not include visualization of flame propagation, and we did not use the possibility of modifying the setup to generate higher mixture turbulence. Furthermore, ignition was performed near the upper flange, which could affect both limit concentrations and the initial stage of near-limit flame propagation. In this work, the setup is upgraded to broaden the scope of experimental research.

The goal of this study is to obtain new insight into turbulent combustion of hydrogen–air mixtures containing water vapor and microdroplets by visualizing flame initiation and propagation in a controlled turbulent flow. Our experimental results constitute a representative database for validating software packages and for developing theoretical models, technological solutions, and safety measures to be used in nuclear power and hydrogen storage engineering.

2. Experimental setup and measurement technique

Figure 1 schematizes the experimental setup used in this study. Its main component, preheated combustion chamber *1*, is a 0.6 m long vertical cylinder of diameter 120 mm.

An aluminum rupture disc is placed between flange 4 and gas outlet 5 to provide for rapid expansion of the mixture under study. The combustion chamber is functionally similar to the high-pressure section of a conventional shock tube.

The setup is equipped with four tubular heating elements (not shown), which are symmetrically mounted on the outer surface of the chamber, parallel to the cylinder axis. With a total heating power of 6 kW, the chamber is heated at a rate of 200 K/h. Tungsten needle

electrodes are placed perpendicular to the axis within the 150 mm long chamber section bounded by perforated plate *2* and blank plate *14*. The pressure inside the chamber is measured with two piezoelectric transducers *6* mounted at its lower end. A pressure transducer placed at gas outlet *5* is used to synchronize measurements with the high-voltage pulse supplied to the spark gap, with a preset time delay. The test mixtures are prepared in fan mixing chamber *13* using a partial pressure technique.

The preparation and experimental procedures used are as described in [24, 25]. Before each experiment, a rupture disc is inserted and a certain amount of water (20–40 ml) is introduced into the chamber. During the preheating stage, the chamber is filled with saturated vapor. After reaching the required pressure p_{V1} (at saturation temperature T_1), the hydrogen–air mixture to be tested is added into the chamber. To prevent condensation and ensure uniform mixing, the premixed gas is introduced in small portions through a heated duct. The rupture disc fails when the pressure p_1 determined by its thickness is reached, and a rarefaction wave begins to propagate down the chamber. A drop in pressure and temperature in the waves incident on and reflected from the blank plate results in partial condensation of the saturated vapor, while additional turbulence is generated between the plates as the mixture flows through perforated plate *2* with an open area ratio of 0.3. Since the vertical extent of the space between the plates is similar to the chamber diameter, and the distance from the spark gap to the perforated plate is equal to the chamber radius, a spark-ignited flame must propagate almost spherically until reaching the walls or the perforated plate. Once the chamber pressure has reached ambient pressure (air at $p_0 = 0.1$ MPa), the mixture of hydrogen, air, vapor, and microdroplets (mist) is ready for ignition. After a preset time delay, a high-voltage pulse is supplied to the spark gap. The disc rupture pressure p_1 varies between 0.2 and 0.7 MPa.

The processes of microdroplet mist formation and flame propagation are visualized through symmetrically located quartz windows with lateral dimensions of 20 mm. High-speed photography is performed by using camera *9*, two Telemar-2 telephoto lenses *10*, and point light source *15*. IR laser diode *11* ($\lambda = 1.56$ μm) combined with photodetector *7* is used to determine droplet concentration as described in [24,25]. The volume fraction of saturated vapor in the mixture of hydrogen, air, vapor, and microdroplets (mist) is calculated by using relations from [24, 25], where predetermined values of p_1 and p_{V1} and a measured liquid-phase volume fraction φ are used as input parameters.

Turbulent fluctuation velocity is evaluated by using schlieren image velocimetry (SIV), which is analogous to the widely used particle image velocimetry (PIV) technique except that density gradients are used as markers instead of seeded particles [26]. Images are processed with PIVLab software [27]. As an example, shown on the left of figure 2 is an image of the velocity vector field in the vicinity of the electrodes immediately before ignition of a 15% $H_2 + 85\%$ air mixture, with a disc rupture pressure of $p_1 = 0.65$ MPa.

A histogram of the distribution of the velocity component u parallel to the chamber axis is shown on the right of figure 2. A similar histogram is obtained for the velocity component perpendicular to the chamber axis. Assuming turbulence isotropy, we can evaluate turbulent fluctuation velocity as $u' = \sqrt{3}\sigma_u$, where the rms deviation σ_u is obtained by processing a sequence of 10–15 images taken over a time interval of at least 1 ms before ignition. In this example, $u' = 1.39$ m/s.

3. Results and discussion

Preliminary experiments on expanding hydrogen-air mixtures not diluted with water vapor have demonstrated that turbulence of certain intensity can be generated in a rarefaction wave. Figure 3 shows images obtained for an initial chamber pressure (disc rupture pressure) of $p_1 = 0.65$ MPa. The spark was fired at 56 ms after the disc ruptured, when the mixture had expanded to ambient pressure. It is clear that the flame structure corresponds to a

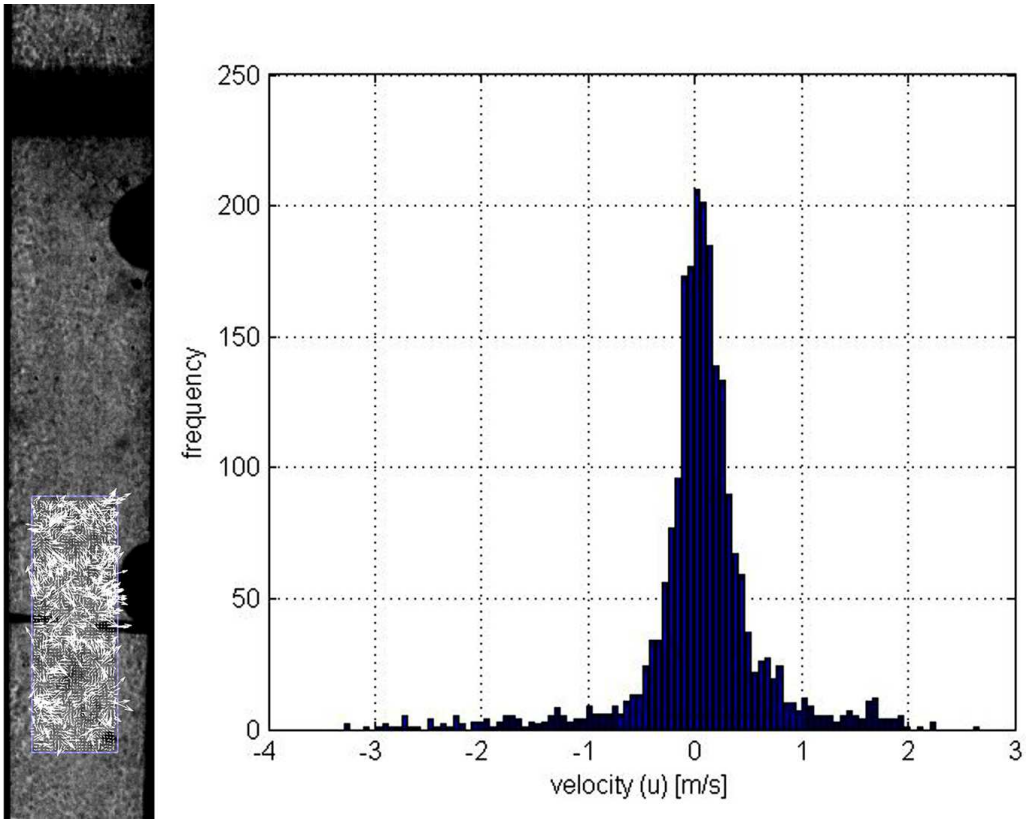

Figure 2. Velocity field before ignition and a histogram of the distribution of the velocity component parallel to the chamber axis.

turbulent combustion regime. Rarefaction waves can be used to create water microdroplets in a combustible gas. Ignition of an expanding vapor–gas cloud simulates a possible nuclear accident scenario.

Optical diagnostics of gas–droplet flow involves increased requirements, particularly regarding light sources. Schlieren images of acceptable quality are obtained for optically dense clouds by employing a DKSSh-150 ultrahigh-pressure xenon lamp as a light source. The captions to the figures below showing experimental results contain information about initial conditions: disc rupture pressure p_1, partial vapor pressure p_{V1} at rupture, and hydrogen–air mixture composition. Also included are the corresponding values of liquid-phase volume fraction φ measured before ignition.

Figure 4 shows the schlieren flow images obtained for a near-flammability-limit mixture at a disc rupture pressure of approximately 0.25 MPa. After ignition, the flame kernel breaks away from the spark gap and moves upwards, driven by buoyancy. Below the spark gap, the mixture begins to burn only after the flame front reaches the perforated plate and additional pressure disturbances are generated. The significant decrease in optical density observed directly behind the flame front can be attributed to rapid droplet evaporation resulting in heat removal from the combustion zone.

As illustrated by figure 5, an increase in hydrogen concentration reduces the amount of condensate. The flame kernel does not break away from the electrodes, and the flame propagates in both directions. An analogous pattern of flame propagation is observed at a higher disc rupture pressure (see figure 6).

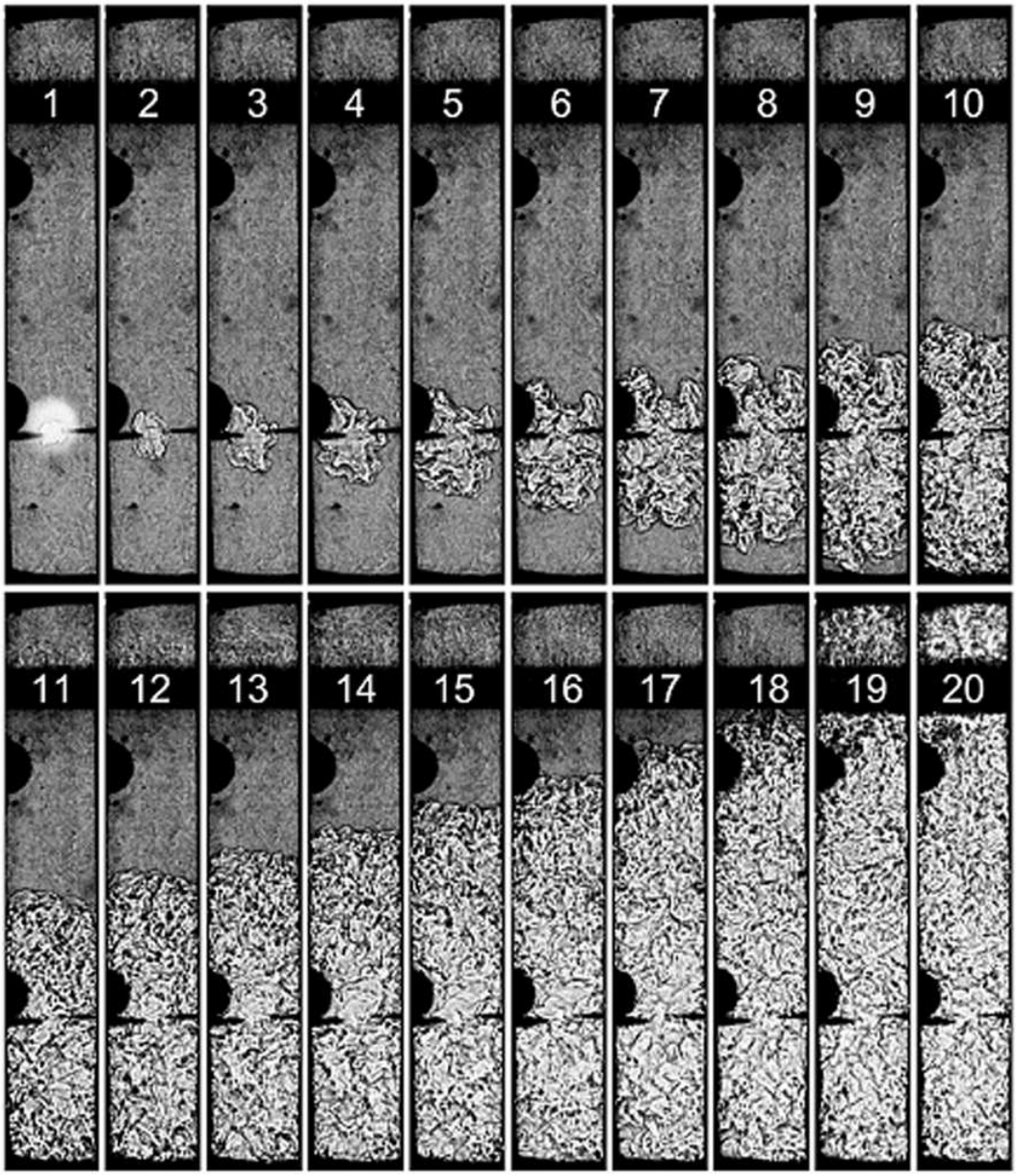

Figure 3. Shadow images of 15% $H_2 + 85\%$ air flame propagation: $p_1 = 0.65$ MPa, $T_1 = 293$ K, $u' = 1.39$ m/s. Time between frames $\Delta t = 0.35$ ms.

An analysis of experimental results suggests that the rapid expansion technique provides an effective means for creating a mixture of hydrogen, air, vapor, and microdroplets (mist). The composition of the two-phase system is determined by the expansion ratio and the concentration of saturated vapor in the initial vapor–gas system. Variation of initial conditions combined with control of droplet size and concentration and schlieren visualization of the flow offers a possibility for investigating flame initiation and propagation processes in a wide range of hydrogen–air mixtures containing water vapor and microdroplets. From a practical perspective, of particular interest is the study of the effect of microdroplets on the flammability limits of hydrogen–air–saturated vapor mixtures.

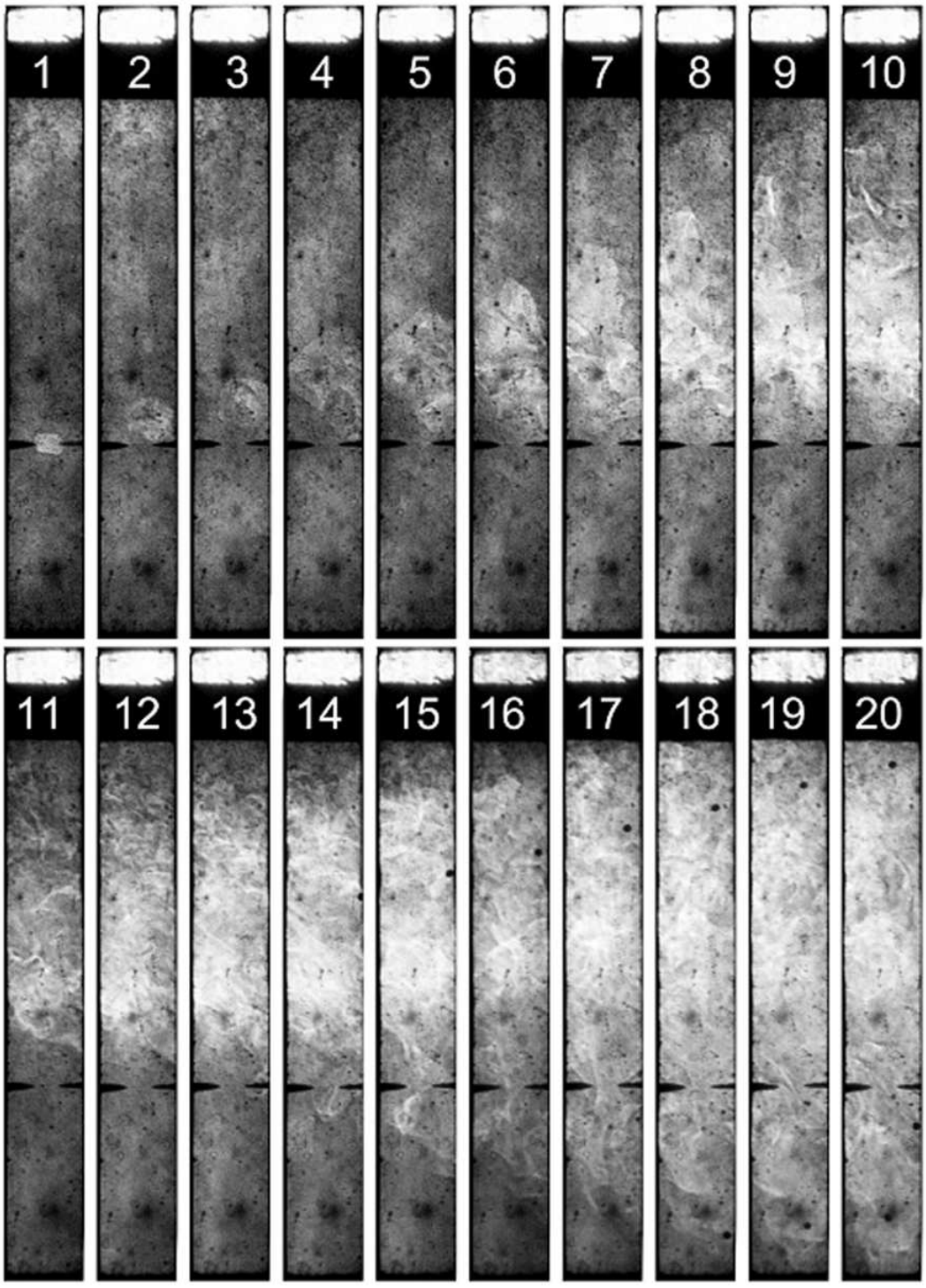

Figure 4. Shadow images of 8.6% H_2 + 91.4% air flame propagation: $p_1 = 0.25$ MPa, $p_{V1} = 0.075$ MPa, $u' = 0.33$ m/s, $\varphi = 9.5 \times 10^{-6}$. Time between frames $\Delta t = 2$ ms.

Figure 7 shows experimental results plotted as a flammability diagram in the coordinates of hydrogen and saturated-vapor volume fractions ($[H_2]$ and $[H_2O]_{vapor}$, vol %). Note that the

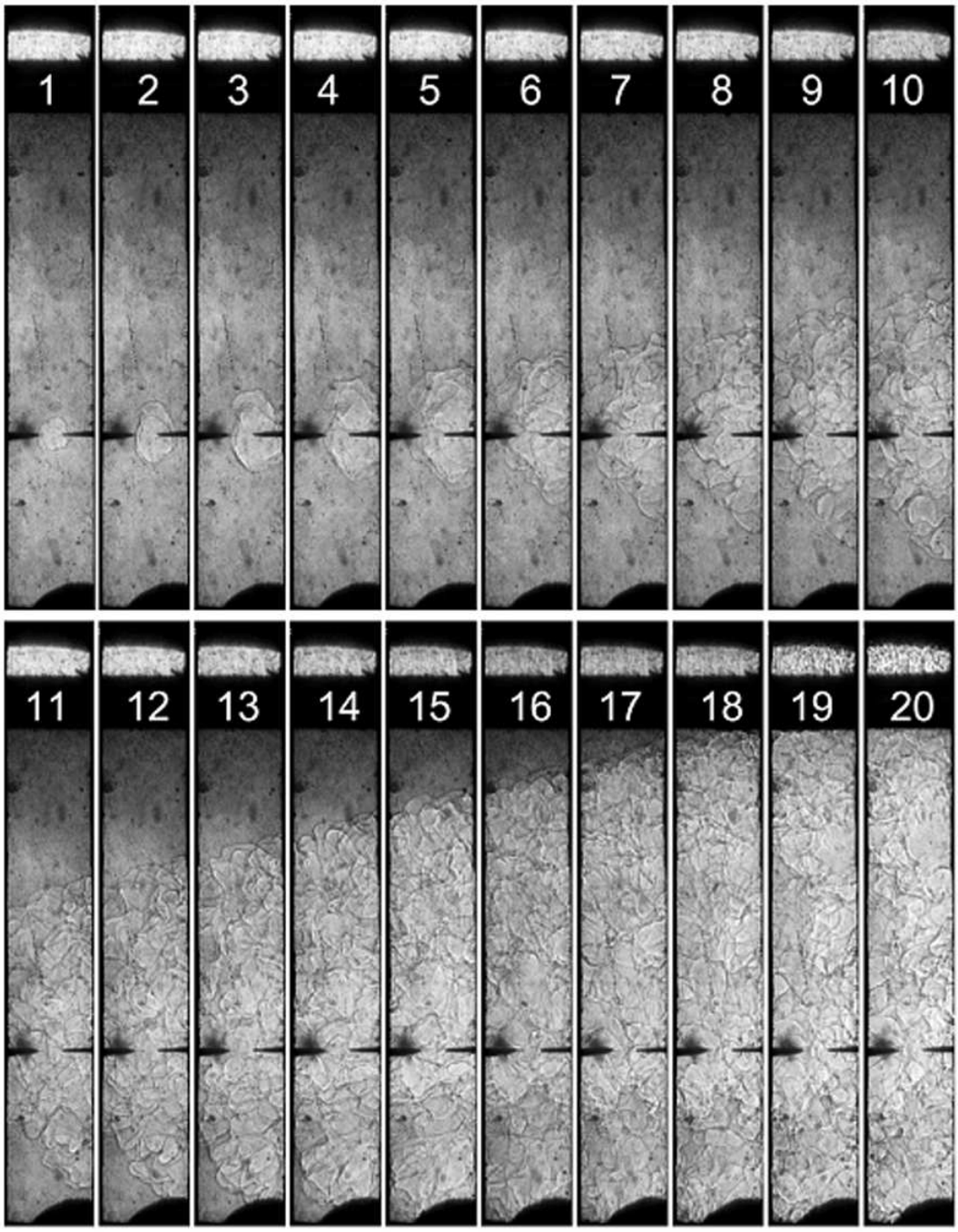

Figure 5. Shadow images of 13.8% H_2 + 86.2% air flame propagation: $p_1 = 0.24$ MPa, $p_{V1} = 0.075$ MPa, $u' = 0.32$ m/s, $\varphi = 4.1 \times 10^{-6}$. Time between frames $\Delta t = 0.432$ ms.

volume percents here are relative to the total volume of the mixture at ignition. Closed squares represent conditions where flame propagation was observed, and open ones correspond to non-flammable mixtures according to [25]. Curves represent the flammability limits of hydrogen–air–saturated-vapor mixtures for upward and downward propagation according to [17]. Results of the present study are represented by red symbols. Comparing them with those reported in [25],

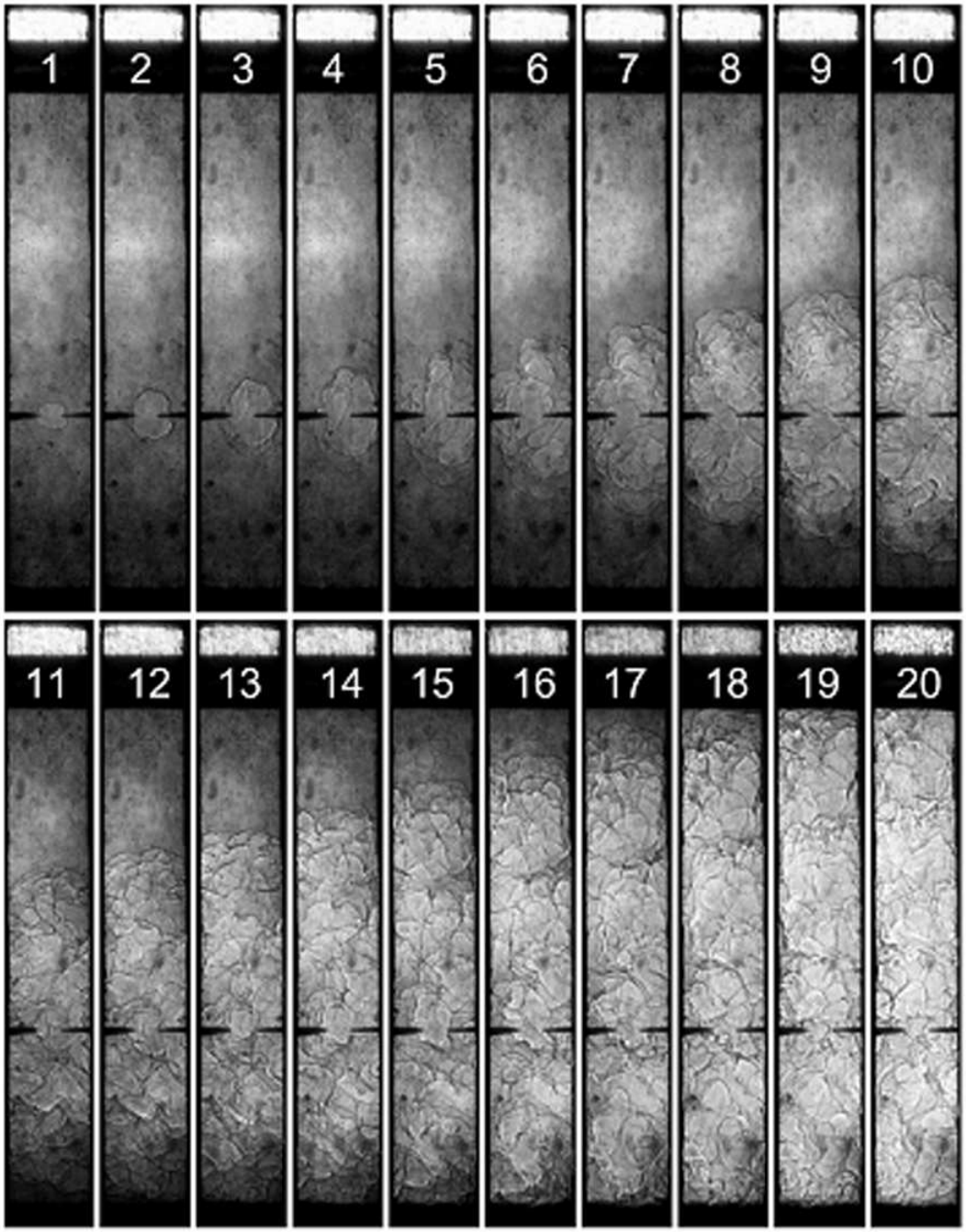

Figure 6. Shadow images of 15.6% H_2 + 84.4% air flame propagation: $p_1 = 0.6$ MPa, $p_{V1} = 0.15$ MPa, $u' = 0.36$ m/s, $\varphi = 7.6 \times 10^{-6}$. Time between frames $\Delta t = 0.32$ ms.

one finds that the liquid-phase volume fraction is lower by a factor of 2 to 3 under the present experimental conditions. This is explained by lower expansion ratio and setup design features. In particular, the use of a perforated plate increases heat transfer to the two-phase flow, leading to faster droplet evaporation. It is clear from figure 7 that the presence of microdroplets with $\varphi < 10^{-5}$ has an insignificant effect on flammability limits.

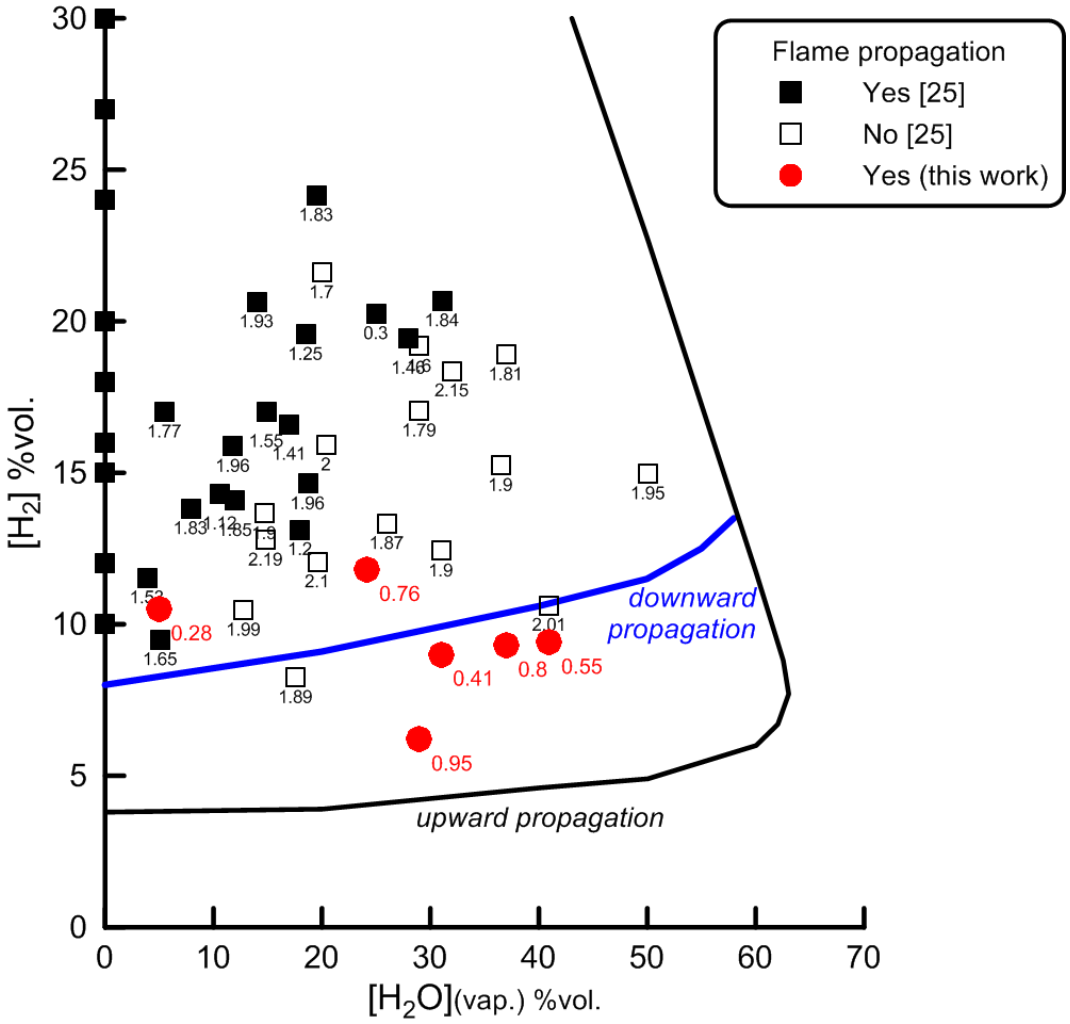

Figure 7. Flammability diagram for mixtures of hydrogen, air, vapor, and microdroplets. Measured liquid-phase volume fractions ($\varphi \times 10^5$) are indicated under symbols.

4. Conclusions

A technique has been developed for evaluating turbulent combustion characteristics in the presence of microdroplets obtained by vapor condensation in the course of rapid expansion. The experimental setup constructed to implement the technique consists of a combustion chamber allowing expansion of the test mixture, a multichannel system for processing signals from pressure transducers mounted along the length of the chamber, and a high-speed imaging system for visualizing flame propagation. The technique includes a method for measuring microdroplet concentration.

Experiments have been conducted to visualize spark-initiated flame propagation through hydrogen–air mixtures at various turbulent intensities, water-vapor volume fractions, and microdroplet concentrations. Turbulent fluctuation velocity is evaluated by using schlieren image velocimetry (SIV) and processing schlieren images obtained before ignition with PIVLab software.

The values of liquid-phase volume fraction measured in these experiments are found to be lower by a factor of 2 to 3 compared to those reported in previous studies. It is shown that the

presence of microdroplets with $\varphi < 10^{-5}$ in a hydrogen–air–vapor system has an insignificant effect on flammability limits.

The new technique can be used to validate software packages designed to simulate emergency conditions at nuclear power plants and provides a basis for new solutions in nuclear safety engineering and hydrogen energy applications.

Acknowledgments

This work was supported by the Federal State Unitary Enterprise "Russian Federal Nuclear Center—Zababakhin All-Russian Research Institute of Technical Physics" (FSUE "RFNC-VNIITF") under contract No. 202-15.

References

[1] Lefebvre A H 1989 *Atomization and Sprays* (New York: Hemisphere)
[2] Green H L and Lane W R 1964 *Particulate Clouds: Dust, Smokes, and Mists* 2nd ed (Princeton, NJ: Van Nostrand)
[3] Kawada H and Mori Y 1973 *Bull. JSME* **16** 1053–1065
[4] Barschdorff D 1975 *Phys. Fluids* **18** 529–535
[5] Sislian J P and Glass I I 1976 *AIAA J.* **14** 1731–1737
[6] Kotake S and Glass I I 1977 *AIAA J.* **15** 215–221
[7] Glass I, Sislian J P and Kalra S P 1977 *AIAA J.* **15** 686–693
[8] Hastings D L and Hodgson J P 1979 *J. Phys. D: Appl. Phys.* **12** 2111–2122
[9] Smolders H J, Willems J F H, de Lange H C and van Dongen M E H 1990 *Current Topics in Shock Waves, 17th Int. Symp. on Shock Waves and Shock Tubes* (*AIP Conf. Proc.* vol 208) pp 802–807
[10] Smolders H J 1992 *Non-linear wave phenomena in a gas-vapour mixture with phase transition* Ph.D. thesis Eindhoven Univ. Technology (Eindhoven, The Netherlands)
[11] Looijmans K N H, Kriesels P C and van Dongen M E H 1993 *Exp. Fluids* **15** 61–64
[12] Looijmans K N H, Willems J F H and van Dongen M E H 1995 *Shock Waves @ Marseille I, Proc. 19th Intl. Symp. on Shock Waves* ed Brun R and Dumitrescu L Z (Berlin, Heidelberg: Springer) pp 215–220
[13] Netseplyaev M I, Lubimova A I, Petrukhin P M and Ploskogolovyi E P 1992 *Mitigation of Coal Dust Explosions in Mines* (Moscow: Nedra)
[14] Mamaev V I, Ibraev G A, Ligai V A, Sheredekin D M and Yatsenko I S 1990 *Prevention of Dust–Methane–Air Explosions* (Moscow: Nedra)
[15] Berman M 1983 Sandia Report SAND 84-0689
[16] Kumar R K and Koroll G W 1992 *Nucl. Saf.* **33** 398–414
[17] Kumar R K 1985 *J. Fire Sci.* **3** 245–262
[18] Marshall B W 1986 Sandia Report SAND 84-0383
[19] Coward H F and Jones G W 1952 *U.S. Bureau of Mines Bull.* 503
[20] Zabetakis M G 1965 *U.S. Bureau of Mines Bull.* 627
[21] Berman M, Sherman M P, Cummings J C, Baer M R and Griffiths S K 1981 Sandia Report SAND 80-2714
[22] Zalosh R G and Bajpai S N 1982 *Hydrogen and Water Reactor Safety* Sandia Report SAND 82-2456 pp 709–726
[23] Tsai S S and Liparulo N J 1982 *Hydrogen and Water Reactor Safety* Sandia Report SAND 82-2456 pp 727–739
[24] Bartenev A M, Gel'fand B E, Medvedev S P, Polenov A N and Khomik S V 2002 *High Temp.* **40** 272–277
[25] Medvedev S P, Gel'fand B E, Polenov A N and Khomik S V 2002 *Combust. Explos. Shock Waves* **38** 381–386
[26] Jonassen D R, Settles G S and Tronosky M D 2006 *Optics Lasers Eng.* **44** 190–207
[27] Thielicke W and Stamhuis E J 2014 *J. Open Res. Softw.* **2** e30